

# Intercalation of salicylic acid into ZnAl layered double hydroxides by ion-exchange and coprecipitation method

M. SILION (FRUNZA), D. HRITCU, M. I. POPA\*

*Department of Chemical Engineering, Faculty of Chemical Engineering and Environmental Protection, Technical University Iasi, Bd. D. Mangeron 71A, 700050, Iasi, Romania*

Salicylic acid was intercalated into an inorganic host consisting of ZnAl-layered double hydroxides lamella by ionic exchange and coprecipitation technique. The precursors and the intercalation compounds were examined by X-ray diffraction (XRD), FTIR spectroscopy, differential thermal and thermo gravimetric analysis and scanning electron microscopy (SEM). Powder X-ray diffractograms show that the basal spacing of the ZnAl layered double hydroxide bearing salicylate as the intergallery anion expanded from 8.7 Å in the precursor to 15.4 Å in ZnAl-layered double hydroxide obtained by ionic exchange and to 14.9 Å in ZnAl-layered double hydroxide prepared by coprecipitation direct method, respectively. The  $\text{NO}_3^-$  peak located at  $1385\text{ cm}^{-1}$  in FTIR spectra of the sample prepared by ion exchange was replaced with peaks characteristic to the intercalated salicylate anion. The thermal stability of the intercalated salicylic acid is significantly enhanced compared with the pure form before intercalation. Using the XRD results combined with a molecular simulation model, a possible representation of the salicylate anion positioning between the lamellar layers has been proposed.

(Received April 10, 2009; accepted April 23, 2009)

**Keywords:** Layered double hydroxide, Ion exchange, Coprecipitation, Intercalation, Salicylic Acid

## 1. Introduction

The class of materials known as layered double hydroxides (LDHs) or hydrotalcite-like materials have the general formula:  $[M_{1-x}^{2+}M_x^{3+}(\text{OH})_2]^{+}A_m^{m-} \cdot z\text{H}_2\text{O}$ , where  $M^{2+} = \text{Mg, Zn, Ca, Co, Fe, Ni, Cu, etc.}$ ,  $M^{3+} = \text{Al, Fe, Cr, Ga, etc.}$ ,  $A^{m-} = \text{Cl}^-, \text{CO}_3^{2-}, \text{NO}_3^-, \text{etc.}$ ,  $m$  is the formal charge of anion and  $x$  is the stoichiometric coefficient that can be varied widely. As it can be seen from the formula, the formal positive charge of the layer depends on the  $M^{2+}/M^{3+}$  ratio. LDHs contain positively charged cations into hydroxide layers, in which the anions are stabilized in order to compensate the positive layer charges.

Layered double hydroxides are currently used in a variety of applications in fields such as catalysis, electronics, photo-chemistry, medicinal chemistry [1-3]. Their most important property is the capacity to exchange the initially intercalated anions with other inorganic or organic simple or complex anions belonging to drugs, dyes, enzymes or polymers.

Due to the ability to exchange the interlayer anion, the layered double hydroxides have been used extensively as biocompatible hosts for several drugs, such as non-steroidal anti-inflammatory agents (NSAID) that are widely used in rheumatism treatment and very often cause adverse secondary effects, such as gastric and duodenal ulcers formation. Several pharmaceutically active compounds such as diclofenac, meclofenamic acid, ibuprofen, ketoprofen, naproxen, etc. have been reversibly intercalated into LDHs for storage and controlled release purposes, as reported in the literature [4-9].

The research efforts were focused in two directions: firstly, the synthesis and characterization of this new category of compounds and secondly the kinetic studies regarding the release of the pharmaceutical active ingredient. The materials containing incorporated drugs within the matrix have been synthesized using traditional nanocomposite preparation techniques: ion exchange, reconstruction and direct coprecipitation. To confirm the compound intercalation into the layered double hydroxide lamella, physical and chemical characterization methods have been used. The second research direction focused mainly upon determining the mechanism and reaction order for the active ingredient release from the matrix and the role played by the pH of the release medium. Various hydrotalcite – medicine composite materials have been studied and reported as drug controlled release formulations [10-15].

Salicylic acid (Sal), also known as 2-hydroxybenzoic acid (as shown in Fig. 7a), is used in rheumatism treatment, but its adverse secondary effects, such as gastric and duodenal ulcer formation are quite common. Salicylic acid has been previously intercalated into MgAl-hydrotalcites containing interlayer chloride anions by reconstruction and coprecipitation methods [16].

In this work we have investigated the intercalation behavior of salicylic acid (Sal), a drug currently used as an anti-inflammatory medication, into ZnAl-hydrotalcite using two synthetic routes: ion-exchange reaction and coprecipitation method.

In the direct ion exchange method, the incorporation of salicylate anions into the LDH is achieved by mixing the LDH with a concentrated Sal solution. The coprecipitation method involves the addition of an

$M^{2+}/M^{3+}$  salt solution to an alkaline solution containing Sal. The solution is then crystallized using the same method as employed in the preparation of the LDH host material [16].

Layered double hydroxides were used because of their capability to prevent taurocholate induced gastric injury in rat was earlier demonstrated and reported in the literature [17] and this is the reason for choosing them as hosts in the present study.

The obtained composites were characterized by powder X-ray diffraction, FTIR spectroscopy, thermal analysis and SEM microscopy.

## 2. Experimental

### 2.1. Materials

All chemicals including  $Zn(NO_3)_2 \cdot 6H_2O$ ,  $Al(NO_3)_3 \cdot 9H_2O$ , NaOH were analytical grade. Salicylic acid was purchased from Aldrich.

### 2.2. Preparation ZnAlLDH

100 ml of an aqueous solution of  $Zn(NO_3)_2 \cdot 6H_2O$  (0.2mol)/ $Al(NO_3)_3 \cdot 9H_2O$  (0.1mol) and an aqueous solution of NaOH 1M, were mixed together by drop wise addition. During the whole process the flow was controlled in such a way that the pH was kept at a constant value of 8.5. The resulting white precipitate was aged at 338 K for 24 h under stirring. After the ageing step, the precipitate was separated by centrifugation, washed extensively with warm de-ionized water until sodium free and dried under vacuum at 40°C.

### 2.3. Preparation of Sal-LDH hybrid materials

*ZnAlLDH intercalated with Sal prepared by ion exchange method (Sal-ZnAl-LDHsi)*

Salicylate – layered double hydroxides nanocomposite samples were prepared by anion exchange reaction using the following procedure: 150 ml of 0.1M Sal aqueous solution were added into 250 ml aqueous dispersion containing 1g ZnAl-LDH under nitrogen atmosphere and vigorous magnetic stirring. The pH of the mixture was held constant at 8.0 by simultaneous addition of 1M NaOH solution. The exchange reaction was allowed to proceed at room temperature for 24 h.

The obtained precipitates were filtered, washed with de-ionized water and dried at 40°C.

*ZnAlLDH intercalated with Sal prepared by direct coprecipitation method (Sal-ZnAl-LDHc)*

A salt solution was prepared by adding 100 mL of de-ionized water to 0.04 mol  $Zn(NO_3)_2 \cdot 6H_2O$  and 0.02 mol  $Al(NO_3)_3 \cdot 9H_2O$ . The solution thus formed was slowly added to an alkaline solution of the drug prepared by dissolving 0.1 mol of salicylic acid (Sal) into 100 mL of water containing a certain amount of 1 M NaOH solution. The required amount of 1 M NaOH was added during addition of the salts solution in order to maintain the pH at

a value close to 8.0. Once the addition was completed the suspension was vigorously stirred under nitrogen atmosphere at 40 °C for 36 hours. The precipitate was centrifuged and washed several times with de-ionized water until the absence of nitrate and potassium ions was confirmed by a conventional method. The product was filtered and dried at 40°C in vacuum atmosphere.

## 2.4. Characterization

Powder X-ray diffraction (XRD) measurements were performed on a Bruckner AXS D8 diffractometer using  $CuK\alpha$  radiation ( $\lambda = 0.154$  nm) at 40 KV and 35 mA between 4° and 70° (2 $\theta$ ) with a graphite secondary monochromator. To confirm the presence of intercalated anions, IR studies were carried out for all samples using a Bomem MB 104 spectrophotometer (4000-400  $cm^{-1}$ ; resolution 4  $cm^{-1}$ , KBr pellet). Thermogravimetric analysis (TG, DTG and DTA) was performed on Mettler-Toledo TGA/SDTA instrument in the temperature range from 25 to 900°C, at a heating rate of 10°C/min under air atmosphere. The molecular modeling studies were carried out using the Hyperchem software package. A Vega Tescan scanning electron microscope was used for SEM morphology analysis. The samples were coated with a thin layer of evaporated carbon for conduction and examined at 30000 kV accelerating voltage.

## 3. Results and discussion

### 3.1. Powder X-ray diffraction (XRD)

The powder XRD patterns of the precursor ZnAl-LDH and the sample produced by reaction of Sal with LDH are shown in Fig. 1. The ZnAl-LDH precursor has an XRD pattern similar to those previously reported [18] for this class of materials, with a basal spacing ( $d_{003}$ ) of 8.7 Å (Fig. 1a). After reaction with Sal, the powder XRD pattern of the product maintains the major characteristic features of ZnAl-LDH. The main diffraction peaks of structure appear at 5.07°, 11.7° and 17.5°, with an expanded basal spacing ( $d_{003}$ ) of 15.4 Å for Sal-ZnAl-LDHsi and of 14.9 Å for Sal-ZnAl-LDHc, respectively (Fig. 1a and 1b). These results are in good agreement with those reported in the literature regarding intercalation of organic anions of similar size to Sal [19, 20]. The diffraction peaks at 15.4 Å and 14.9 Å are assigned the  $d_{003}$ , proving that the guest molecules are lying horizontally to the hydroxide region in a monolayer. The ZnAlLDH\_SALsi peak at 17.5° 2 $\theta$  might be the reflection of the unchanged LDH precursor; this indicating that there is very little of the unexchanged LDH-nitrate phase left in the product. The peak at 11.7° 2 $\theta$  is the superposition of (003) reflection of the precursor and (006) reflection of the intercalation product, accounting for its enhanced intensity.

The intercalation of Sal anions inside the lamellar host structure is thus clearly evidenced in all the cases by the basal spacing net increase in the composite organic - inorganic derivatives.

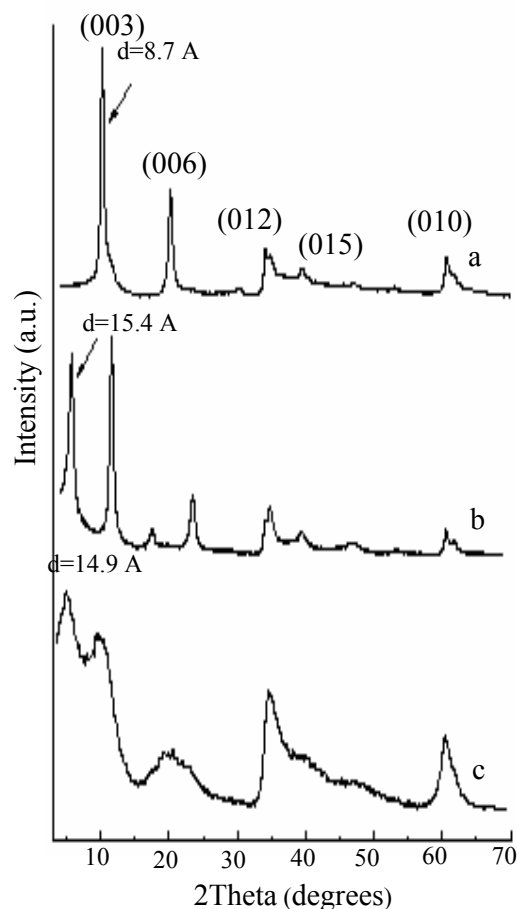


Fig. 1. The XRD spectra (a) ZnAl LDH, (b) Sal-ZnAl-LDHsi, (c) Sal-ZnAl-LDHc

The reflections can be indexed to a hexagonal lattice with R-3m rhombohedral symmetry, commonly used for the description of the LDH structures. The unit cell parameter,  $a$ , is the average distance between two metal ions in the layers and  $c$  is three times the distance from the center of one layer to the next. The value of  $a$  ( $=2d_{110}$ ) is a function of the average radii of the metal cations whilst the value of  $c$  ( $=3d_{003}$ ) is a function of their average charge, the nature of the interlayer anion and the water content. The parameter  $a$  value of 3.06 Å and  $c$  of 26.2 Å are close to the values previously reported for ZnAl-LDH [21]. After the intercalation of Sal, the value of parameter  $c$  increases due the replacement of nitrate anions with Sal anions. Table 1 lists the gallery height and lattice parameters for precursor and Sal-LDHs.

Table 1. Lattice parameters and gallery height.

| Sample         | $d_{003}$ (Å) | $c$ (Å) | $a$ (Å) | Gallery height (Å) |
|----------------|---------------|---------|---------|--------------------|
| ZnAl-LDH       | 8.7           | 26.2    | 3.06    | 3.9                |
| Sal-ZnAl-LDHsi | 15.4          | 46.2    | 3.058   | 10.6               |
| Sal-ZnAl-LDHc  | 14.9          | 44.6    | 3.056   | 10.1               |

|                |      |      |       |      |
|----------------|------|------|-------|------|
| ZnAl-LDH       | 8.7  | 26.2 | 3.06  | 3.9  |
| Sal-ZnAl-LDHsi | 15.4 | 46.2 | 3.058 | 10.6 |
| Sal-ZnAl-LDHc  | 14.9 | 44.6 | 3.056 | 10.1 |

### 3.2 FTIR spectroscopy

The intercalation of Sal in the lamella of ZnAl-LDH is also confirmed by FTIR spectroscopy (Fig 2). All the vibration bands of the organic anion are observed together with the absorption bands of ZnAl-LDH.

The FTIR spectrum of the ZnAl-LDH is shown in Fig 2a. The absorption band at around 3431  $\text{cm}^{-1}$  is attributed to the OH stretching due to the presence of hydroxyl group of LDH and/or physically adsorbed water molecules. The appearance of a strong band at 1381  $\text{cm}^{-1}$  can be assigned to the  $\nu_3$  nitrate group, the counter anion in the ZnAl-LDH. The band at 1626  $\text{cm}^{-1}$  is due to  $\nu(\text{H-O-H})$  band vibration. As shown in Fig. 2a, ZnAl-LDH is free of carbonate anion. The bands in the low frequency region correspond to the lattice vibration modes such as the translation vibrations of Zn-OH at 611  $\text{cm}^{-1}$  and Al-OH at 790  $\text{cm}^{-1}$  and 554  $\text{cm}^{-1}$  respectively, and the deformation vibration of HO-Zn-Al-OH at 431  $\text{cm}^{-1}$  and of Al-OH around 936  $\text{cm}^{-1}$  which are typical for this class of materials [22-25].

The FTIR spectrum of pure Sal shows many absorption bands (Fig.2b). In addition to bands at high wave number values, due to  $\nu(\text{OH})$  and  $\nu(\text{=C-H})$  moieties, a band is recorded at 1651  $\text{cm}^{-1}$ , due to mode  $\nu(\text{C=O})$  of the acid group; the abnormally low intensity of this band is due to the presence of intramolecular hydrogen bonds. The bands due to  $\nu(\text{C-C})$  of the aromatic ring are recorded at 1583, 1485, and 1467  $\text{cm}^{-1}$ ; those due to modes  $\nu(\text{C-O})$  and  $\delta(\text{O-H})$  of the acid and alcohol functions are recorded at 1296, 1240, and 1290  $\text{cm}^{-1}$ , while in-plane and out-of-plane  $\delta(\text{CH})$  bands are recorded below 1000  $\text{cm}^{-1}$  [26].

The spectrum recorded after incorporation of the Sal into lamella of ZnAl-LDH is presented in Fig.2c and 2d. The FTIR spectrum of Sal-ZnAl-LDH contains both the characteristic peaks of pure Sal and the typical peak of LDHs, which indicates that the Sal anions have been intercalated into the interlayer galleries of the LDHs. Due to the ionization of the acid group, the band previously detected for free Sal at 1651  $\text{cm}^{-1}$  disappears, while a new band is recorded at 1570  $\text{cm}^{-1}$ . The appearance of this band is caused by the  $\nu_{\text{as}}(\text{COO}^-)$  mode.

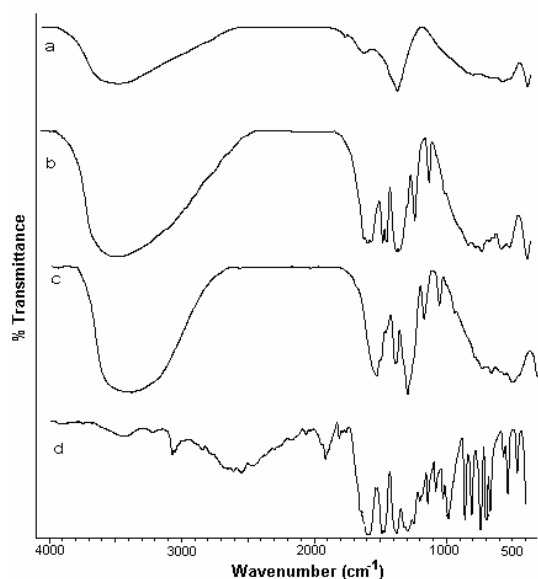


Fig. 2. FTIR spectra (a) ZnAl LDH, (b) Sal, (c) Sal-ZnAl-LDHsi (d) Sal-ZnAl-LDHc

Another band recorded at  $1364\text{ cm}^{-1}$  is due to the symmetric vibration  $\nu_s(\text{COO}^-)$ . The band originated from the  $\delta(\text{CH}_3)$  mode is recorded at  $1386\text{ cm}^{-1}$ .

The band assigned to the nitrate group ( $1381\text{ cm}^{-1}$ ) had lower intensity after the ion-exchange reaction, supporting the assumption that  $\text{NO}_3^-$  anion was replaced by Sal. The other bands are recorded in positions very close to those previously shown for free Sal. In addition, bands due to Zn-Al-OH translational modes are recorded.

### 3.3 Thermal stability

The TG and DTG curves of the precursors Sal, ZnAl-LDH and the composites Sal-ZnAl-LDHs are depicted in Fig. 3-6.

The TG-DTG curves for Sal (Fig.3) exhibit two major stages of weight loss process until the temperature of  $460^\circ\text{C}$ . These steps can be attributed to the combustion of Sal.

Fig.4 shows the thermogravimetric analysis and differential thermal analysis curves of the host LDH. Thermal decomposition of LDHs is dependent on the nature of the layer cations, the nature of the interlayer anion, and the experimental conditions during analysis. The ZnAl-LDH sample presents four weight loss stages. The first occurs up to  $182^\circ\text{C}$  corresponding to the removal of surface and the interlayer water molecules; they are quite strongly attached to the hydroxide layer and/or interlayer anion via hydrogen bonds and the interlayer

balancing anion  $\text{NO}_3^-$ . The next steps, up to  $565^\circ\text{C}$ , are due to dehydroxylation of the ZnAl-LDH basal layer as well as decomposition of nitrate anions.

The TG curve of Sal-LDHs (Fig.5 and Fig.6) clearly shows a rapid weight loss occurring between  $230^\circ$  and  $430^\circ\text{C}$ . This event is attributed to the decomposition of the Sal intercalated and to the dehydroxylation of ZnAl-LDH. From TG curve it is easily observed that the mass loss in the region  $350\text{-}500^\circ\text{C}$  is 20.3% for Sal-ZnAlLDHsi and 22.5% for Sal-ZnAl-LDHc, respectively. This event corresponds to a total combustion of the organic component.

Furthermore, it is noted that Sal anions were completely decomposed above  $420^\circ\text{C}$ , a higher value than the decomposition temperature of raw salicylic acid. This proves the enhanced thermal stability of intercalated Sal due to the host-guest interaction between lamella of ZnAl-LDH.

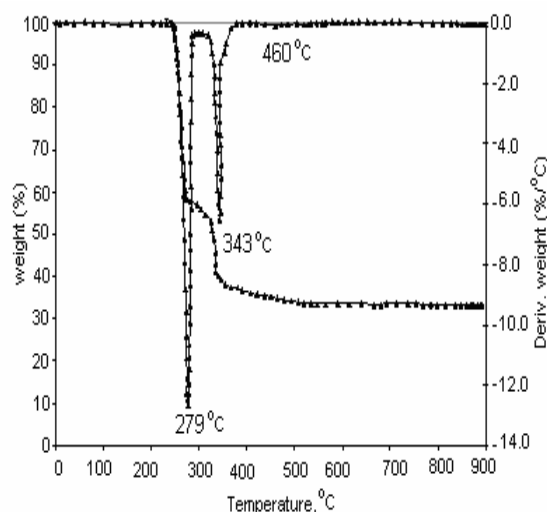


Fig.3.The TG-DTG analysis of SAL.

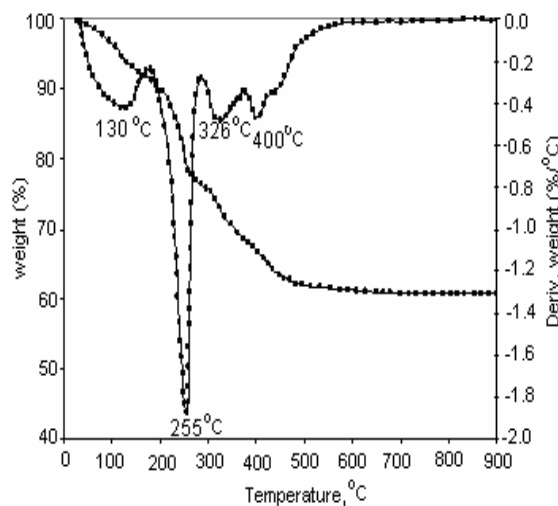


Fig.4.The TG-DTG analysis ZnAl-LDH.

The thermal degradation stages and the weight loss recorded during the analysis of the precursors and the Sal containing compounds are presented in Table2.

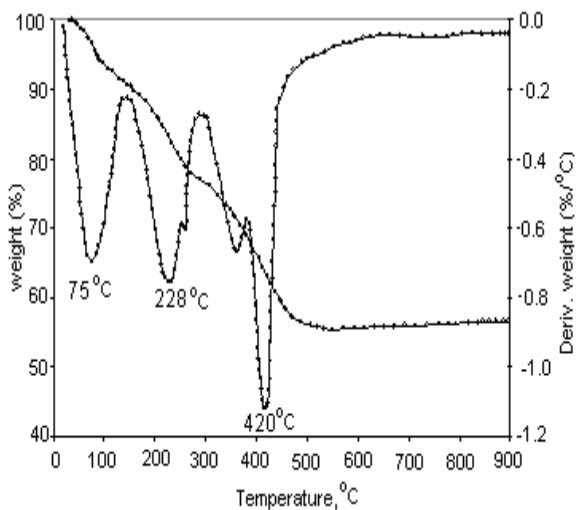


Fig.5.The TG-DTG analysis Sal-ZnAl-LDHsi

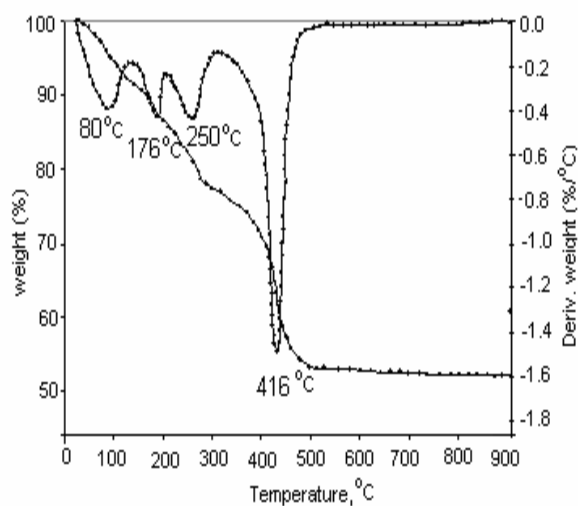


Fig.6.The TG-DTG analysis Sal-ZnAl-LDHc

Table 2. The thermogravimetric parameters for Sal, ZnAl-LDH and the new inorganic – organic hybrid structures obtained by intercalation of salicylate between the layers of layered double hydroxides (LDHs)

| Sample cod     | Stage 1 <sup>a</sup>             |                                  |                    | Stage 2 <sup>b</sup>             |                                  |                    | Stage 3 <sup>c</sup>             |                                  |                    | Stage 4 <sup>d</sup>             |                                  |                    | Char yield (%) |
|----------------|----------------------------------|----------------------------------|--------------------|----------------------------------|----------------------------------|--------------------|----------------------------------|----------------------------------|--------------------|----------------------------------|----------------------------------|--------------------|----------------|
|                | T <sub>i</sub> <sup>e</sup> (°C) | T <sub>f</sub> <sup>f</sup> (°C) | W <sup>g</sup> (%) | T <sub>i</sub> <sup>e</sup> (°C) | T <sub>f</sub> <sup>f</sup> (°C) | W <sup>g</sup> (%) | T <sub>i</sub> <sup>e</sup> (°C) | T <sub>f</sub> <sup>f</sup> (°C) | W <sup>g</sup> (%) | T <sub>i</sub> <sup>e</sup> (°C) | T <sub>f</sub> <sup>f</sup> (°C) | W <sup>g</sup> (%) |                |
| ZnAl-LDH       | 30                               | 182                              | 8.74               | 182                              | 287                              | 14.82              | 287                              | 373                              | 7.69               | 373                              | 677                              | 8.07               | 60.68          |
| Sal            | 249                              | 304                              | 44.15              | 304                              | 380                              | 18.69              | 380                              | 565                              | 4.03               | -                                | -                                | -                  | 33.13          |
| Sal-ZnAl-LDHc  | 30                               | 145                              | 9.33               | 145                              | 289                              | 13.75              | 289                              | 613                              | 21.55              | -                                | -                                | -                  | 55.37          |
| Sal-ZnAl-LDHsi | 20                               | 134                              | 8.86               | 134                              | 199                              | 4.92               | 199                              | 322                              | 11.07              | 322                              | 600                              | 24.6               | 50.55          |

<sup>a</sup> First process of the compound decomposition; <sup>b</sup> Second process of the compound decomposition; <sup>c</sup> Third process of the compound decomposition; <sup>d</sup> The last process of the compound decomposition <sup>e</sup> Initial temperature of a decomposition process; <sup>f</sup> Final temperature of a decomposition process; <sup>g</sup> Weight loss of the compounds after the end of a decomposition process.

The total loss was 38.5 % in the case of the LDH as a reference sample, 49.5 % for Sal-ZnAl-LDHsi and 45% for Sal-ZnAl-LDHc, respectively.

The presence of micro pores is confirmed on DTG plots. Indeed the adsorbed water molecules desorption from intercalates appear as two separate events for Sal-ZnAl-LDHs and as a continuous step for ZnAl-LDH.

### 3.4. Structural modeling

The molecular dimension of Sal compound, calculated using the chemical bond lengths and atomic angles (using Hyperchem software), is 5.12 Å along the y-axis and 6.6 Å along the x-axis.

Given the 0.48 nm thickness of the Zn-Al layer [27], the interlayer spacing was estimated from  $d_{003}$  at 15.4 Å for Sal-ZnAl-LDHsi and 14.9 Å for Sal-ZnAl-LDHc, both values being larger than the molecular size of Sal determined with Hyperchem software. The result suggests a vertically positioned bilayer orientation of Sal molecules between the layers, with the carboxylate ions pointing alternatively to the neighboring hydroxide groups in a similar manner to intercalated 5-aminosalicylic acid, as reported in earlier studies [28]. The model also takes into account the length of the hydrogen bonds established between the anions and the LDH hydroxyl groups. Based on these data, a schematic model of ZnAl-LDH and Sal-ZnAl-LDHs as shown in Fig. 7 is proposed.

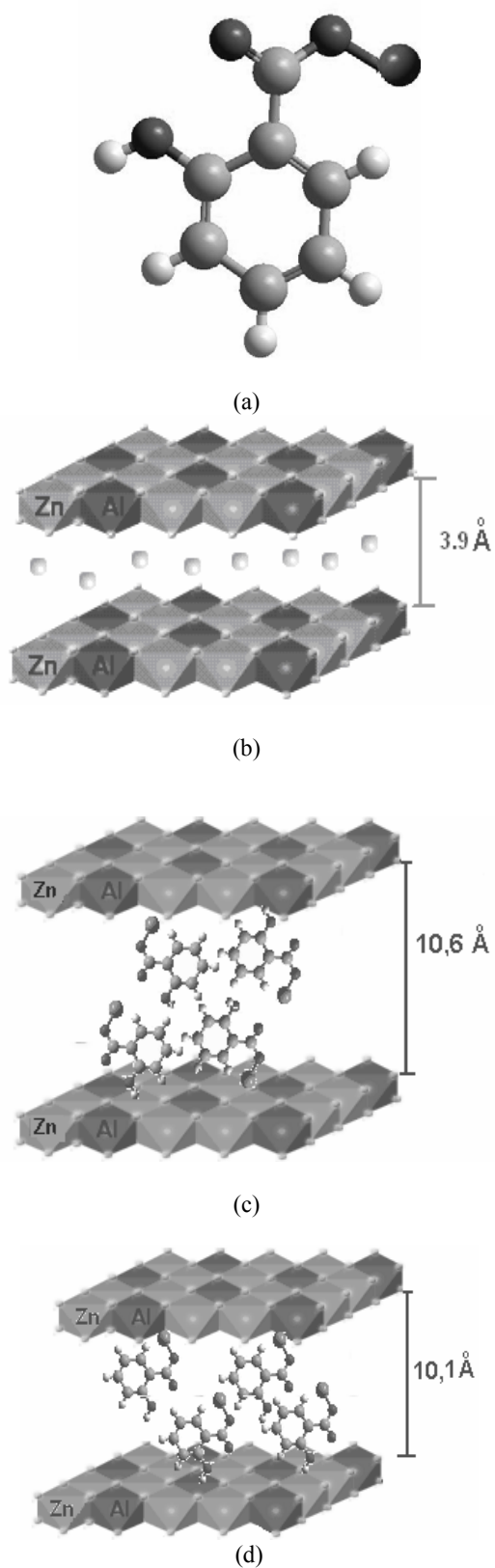


Fig. 7. Structure of Sal and schematic models of the Sal intercalation into LDHs: (a) salicylic acid, (b) ZnAl-LDH, (c) Sal-ZnAl-LDHsi, (d) Sal-ZnAl-LDHc

### 3.5. SEM

The morphologies of ZnAl-LDH and Sal-LDHs obtained by SEM are presented in Fig. 8.

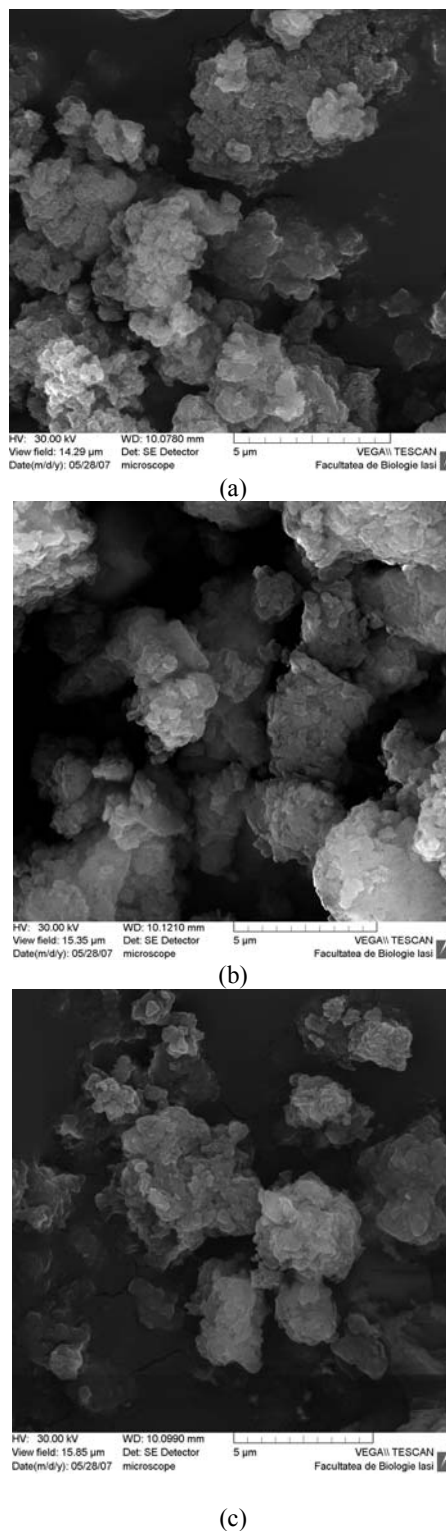


Fig. 8. SEM micrograph for (a) ZnAl-LDH, (b) Sal-ZnAl-LDHsi, (c) Sal-ZnAl-LDHc

Sal-LDHs show typical composite morphology, with non-uniform irregular agglomerates of compact and non-porous plate-like structures similar to the morphology of ZnAl-LDHs with intercalated sodium dodecyl sulfate or  $\alpha$ -naphthaleneacetate [19, 30].

#### 4. Conclusions

Sal-LDHs were obtained by intercalation of Sal anions into zinc-aluminium layered double hydroxide by ion exchange reaction and coprecipitation method. XRD diffractometry and FTIR spectroscopy methods confirm the intercalation of Sal anions into lamella of ZnAl-LDH structure. The recorded basal spacing was 8.7 Å for simple LDHs.

Upon incorporation of salicylic acid into zinc hydroxide layer, the intercalative monohybrid had a basal spacing of 15.4 Å for Sal-ZnAl-LDHsi and 14.9 Å for Sal-ZnAl-LDHc, respectively. The expansion is due to the need to accommodate the Sal anion with a specific orientation and a larger size than nitrate, as indicated by its molecular structure. In the FTIR spectra, the band characteristic for nitrate group has disappeared due its replacement with Sal anions. The thermal stability of Sal was improved by intercalation.

A structural model for intercalates has been proposed based on optimized geometry of Sal. The anions are accommodated in the interlayer region as a bilayer with the carboxylate groups interacting simultaneously with both upper and lower hydroxide layers belonging to LDHs.

#### Acknowledgments

Funding for this research project was provided by the Ministry of Science and Education, under CEEEX grant 108/2006. We are grateful to dr. Raileanu Dumitru for the help with SEM analysis.

#### References

- [1] S. Kannan, A. Dubey, H. Knozinger, J. Catal. **231**, 381(2005)
- [2] A. Vaccari, Appl. Clay Sci. **14**, 161 (1999).
- [3] U. Costantino, M. Nocchetti, Nova Science Publishers, New York (2001).
- [4] V. Ambrogi, G. Fardella, G. Grandolini, L. Perioli, Int. J. Phar. **220**, 23 (2001).
- [5] M. Del Arco, E. Cebadera, S. Gutierrez, C. Martin, M. J. Montero, V. Rives, J. Rocha, M. A. Sevilla, J. Pharm. Sci. **93**, 6, 1649 (2004a).
- [6] M. Del Arco, A. Fernandez, C. Martin, V. Rives, Appl. Clay Sci. **42**, 538 (2009).
- [7] Z. Wang, E. Wang, L. Gao and L. Xu, J. Solid State Chem. **178**, 736 (2005).
- [8] H. Zhang, K. Zou, H. Sun, X. Duan, J. Solid State Chem. **178**, 3485 (2005).
- [9] S. H. Hwang, Y. S. Han and J. H. Choy, Bull. Korean. Chem. Soc. **22**, 1019 (2001).
- [10] M. Frunza, G. Lisa, R. Zonda, M. I. Popa, Rev. Chim. **59**, 409 (2008).
- [11] M. Del Arco, S. Gutiérrez, C. Martín, V. Rives, J. Rocha, J. Solid State Chem. **177**, 3954 (2004).
- [12] F. P. Bonina, M. L. Giannossi, L. Medici, C. Puglia, V. Summa, F. Tateo, Appl. Clay Sci. **41**, 165 (2008).
- [13] U. Constantino, V. Ambrogi, M. Nocchetti, L. Perioli, Micropor. Mesopor. Mat. **107**, 149 (2008).
- [14] B. Li, J. He, D. G. Evans, X. Duan, Appl. Clay Sci., **27**, 199 (2004).
- [15] A. I. Khan, L. Lei, A. J. Norquist, D. O'Hare, Chem. Commun. 2342 (2001).
- [16] M. Frunza, G. Carja, M. I. Popa, Scientific Study and Research, **VI**, 173 (2005).
- [17] S. Carlino, Solid State Ionics, **98**, 73 (1997).
- [18] B. P. Yu, J. Sun, M. Q. Li, H. S. Luo, J. P. Yu, World J. Gastroenterol. **9**, 1427 (2003).
- [19] Z. P. Xu, H. C. Zeng, J. Phys. Chem. B, **105**, 1743 (2001).
- [20] M. Z. Hussein, Z. Zainal, A. H. Yahaga, J. Contr. Rel. **82**, 417 (2002).
- [21] S. Aisawa, S. Takahashi, W. Ogasawara, Y. Umetsu, E. Narita, J. Solid State Chem. **162**, 52 (2001).
- [22] V. Ambrogi, G. Fardella, G. Grandolini, L. Perioli, Int. J. Phar. **220**, 23 (2001).
- [23] S. Velu, V. Amukumar, V. Narayanan, C. S. Swamy, J. Mat. Sci., **32**, 957 (1997).
- [24] S. Kanan, C.S. Swamy, J. Mat. Chem. Lett. **11**, 1585 (1992).
- [25] M. Z. Hussein, W.L. Chan, Mat. Chem. **85**, 427 (2004).
- [26] F. Li, L.H. Zhang, D.G. Evans, C. Forano, X. Duan, Thermochim. Acta, **424**, 15 (2004).
- [27] L. J. Bellamy, The Infrared Spectra of Complex Molecules, Chapman and Hall, London, (1975).
- [28] F. Cavani, F. Trifiro, A. Vaccari, Catal. Today, **11**, 173 (1991).
- [29] H. Zhang, K. Zou, H. Sun, X. Duan, J. Solid State Chem. **178**, 3485 (2005).
- [30] L. Raki, J.J. Beaudoin, L. Mitchell, Cem. Concr. Res. **34**, 1717 (2004).
- [31] M.Z. Hussein, Z. Zainal, Y. M. Chin, J. Mater. Sci. Lett. **19**, 879 (2000).

\*Corresponding author: mipopa@ch.tuiasi.ro